Does $H \to \gamma\gamma$ taste like vanilla new physics?

L. G. Almeida,[a] **E. Bertuzzo,**[a] **P. A. N. Machado**[a,b] **and R. Zukanovich Funchal**[a,b]

[a]*Institut de Physique Théorique, CEA-Saclay,*
91191 Gif-sur-Yvette, France
[b]*Instituto de Física, Universidade de São Paulo,*
C. P. 66.318, 05315-970 São Paulo, Brazil
E-mail: leandro.almeida@cea.fr, enrico.bertuzzo@cea.fr,
accioly@fma.if.usp.br, zukanov@if.usp.br

ABSTRACT: We analyse the interplay between the Higgs to diphoton rate and electroweak precision measurements constraints in extensions of the Standard Model with new uncolored charged fermions that do not mix with the ordinary ones. We also compute the pair production cross sections for the lightest fermion and compare them with current bounds.

Contents

1 Introduction

The Standard Model (SM) has been so far exhaustedly ratified by experiments. The recent discovery of a new boson, compatible with the SM Higgs particle, reported by ATLAS [1] and CMS [2] experiments at the Large Hadron Collider (LHC), finally inaugurates a new era in the field. For the first time we have access to the electroweak symmetry breaking sector of the SM and to the mysteries it may reveal.

Indeed, the combined analyses [3–5] of ATLAS and CMS results at 7 and 8 TeV [6–10] with the Tevatron experiments data [11], seem to suggest that physics beyond the SM is already here. There are two important facts that all these analyses seem to indicate: the gluon-gluon Higgs production cross section is $\sim 40\%$ smaller and the Higgs to diphoton decay ~ 3 larger than the SM prediction. Furthermore, the CMS uncombined Higgs data [2] clearly corroborate to this assessment. Their $H \to \gamma\gamma$ events tagged as produced by vector boson fusion prefer a production cross section ~ 2 times higher than the SM value, while their $H \to \gamma\gamma$ untagged events prefer it only $\sim 50\%$ higher. The former can be explained by an increase of $\Gamma(H \to \gamma\gamma)$ whereas the latter by an additional decrease of the gluon-gluon Higgs production cross section. Their $H \to ZZ$ events also point towards a $\sim 30\%$ lower gluon-gluon cross section.

In this paper we focus on the Higgs to diphoton decay as a possible smoking gun to new physics. The $H \to \gamma\gamma$ partial decay width, which appear only at loop level, is sensitive to the existence of extra charged states that couple to the Higgs boson. Such

states arise in a variety of beyond the SM models. Thus, since the first measurements by the LHC experiments suggested the observed Higgs to diphoton rate was larger than the SM one [12, 13], a number of works have studied the effect of new particles in this width [14–26].

We propose here to map, in a model independent fashion, the properties (masses, charges, couplings) that the new particles have to satisfy in order to account for the observed $H \to \gamma\gamma$ width in an economic way and pass the electroweak precision tests. We consider the effect of extra fermions, in their smallest allowed $SU(2)_L \times U(1)_Y$ representations, assuming that possible additional states, that could accompany these fermions in a complete model, are sufficiently heavy to play no significant role. We also compute, in each case, their production cross section at the LHC and discuss possible signatures and limits.

This work is organized as follows. In the section 2 we present the general framework of our approach to the $H \to \gamma\gamma$ width and in section 3 we discuss the doublet-singlet and triplet-doublet uncolored fermion states and their corresponding lagrangians that we introduced in order to increase the diphoton rate (the specific choice $y = 1/2$ for the doublet hypercharge in the triplet-doublet model corresponds to the supersymmetric Wino-Higgsino case). In section 4 we discuss what kind of enhancements are possible with these models and their dependency on the model parameters. In section 5 we examine the constraints on the parameter space from the electroweak precision tests. In section 6 we consider the predictions for the pair production cross sections of these new fermions at the LHC operating at a center of mass energy of 8 TeV.

2   General framework

We assume the new 125 GeV particle observed at the LHC is in fact a SM-like Higgs boson, responsible for the electroweak symmetry breaking. It is a fundamental scalar transforming as part of the $SU(2)_L$ doublet

$$H = \begin{pmatrix} h^+ \\ h^0 \end{pmatrix}, \tag{2.1}$$

with the SM Higgs charge assignments and hypercharge Y=1/2.

The new particles will not mix with the SM fermions, they will only couple to the Higgs and the gauge sector respecting the SM symmetry group. This is feasible in a concrete model by introducing a new quantum number in connection to an unbroken or nearly unbroken symmetry, exclusive to the new sector. We will consider colorless fermion states in their lowest allowed $SU(2)_L \times U(1)_Y$ representations, i.e. singlets, doublets and triplets. Once the representation is chosen, their couplings with the SM gauge boson will be basically fixed. The only free parameters will be their couplings to the Higgs, their charges and their masses. We do not study here particles with $SU(3)_C$ quantum numbers, for simplicity and because we are not interested in this work to change the Higgs production cross section.

We will examine the allowed regions of these parameters in order for these new particles to significantly contribute to the Higgs diphoton width. We will do this by imposing $1.4 < \Gamma(H \to \gamma\gamma)/\Gamma^{SM}(H \to \gamma\gamma) < 5.4$ at 95% CL [3].

The Higgs to diphoton decay can be written in terms of the couplings to the particles in the loop as

$$\Gamma(H \to \gamma\gamma) = \frac{\alpha^2 m_H^3}{1024\pi^3} \left| \frac{2}{v} A_1(\tau_W) + \frac{8}{3v} A_{1/2}(\tau_t) + \frac{2g_{Hf\bar{f}}}{m_f} N_{c,f} q_f^2 A_{1/2}(\tau_f) + \frac{g_{HSS}}{m_S^2} N_{c,S} q_S^2 A_0(\tau_S) \right|^2,$$

(2.2)

where $\tau_a \equiv (m_H/2m_a)^2$, $a = W, t, f, S$, m_H is the Higgs mass, f (S) is a generic new fermion (scalar) with electric charge q_f (q_S), in units of the electric charge e, number of colors $N_{c,f}$ ($N_{c,S}$) and mass m_f (m_S), coupling to the Higgs with strength $g_{Hf\bar{f}}$ (g_{HSS}). The loop functions A_1, $A_{1/2}$ and A_0 are defined in the appendix.

The first and second contributions are the dominant SM ones, while the others are possible contributions from extra fermions and scalars. Since for the W boson contribution $A_1(\tau_W) \simeq -8.3$ and for the top quark $A_{1/2}(\tau_t) \simeq +1.8$, to increase $H \to \gamma\gamma$ we need to include a new negative contribution, comparable to the top one.

It was shown in ref. [23], where the leading contributions from new particles to the diphoton decay width was derived from the QED beta functions, that for fermions carrying the same electric charge and described by the mass matrix M_f

$$\frac{2g_{Hf_i\bar{f}_i}}{m_{f_i}} = \frac{\partial}{\partial v} \log m_{f_i}^2(v),$$

(2.3)

where $m_{f_i}^2(v)$ is an eigenvalue of $M_f^\dagger M_f$. Clearly if fermions cannot mix they will all contribute to the loop with the same sign of the top contribution and decrease the Higgs to diphoton width. So a required condition to enhance the diphoton coupling to the Higgs is to have mixture. In this case the off-diagonal elements can enter with a term carrying the same sign of the W contribution, cancelling the top and increasing the width.

However, any physics beyond the SM must face its tremendous success: fulfill the electroweak precision tests and evade direct detection bounds.

New states will inevitably contribute to the vacuum polarization amplitudes of the electroweak gauge bosons $\Pi_{ab}^{\mu\nu}(q^2) = -ig^{\mu\nu}\Pi_{ab}(q^2) + q^\mu q^\nu$ terms [27, 28]. These new physics effects can be parametrized by the so-called quantum oblique parameters S, T and U defined as [28]

$$\alpha(M_Z^2) S^{\mathrm{NP}} = \frac{4s_W^2 c_W^2}{M_Z^2} \left[\Pi_{ZZ}^{\mathrm{NP}}(M_Z^2) - \Pi_{ZZ}^{\mathrm{NP}}(0) - \Pi_{\gamma\gamma}^{\mathrm{NP}}(M_Z^2) - \frac{c_W^2 - s_W^2}{c_W s_W} \Pi_{\gamma Z}^{\mathrm{NP}}(M_Z^2) \right]$$

$$\alpha(M_Z^2) T^{\mathrm{NP}} = \frac{\Pi_{WW}^{\mathrm{NP}}(0)}{M_W^2} - \frac{\Pi_{ZZ}^{\mathrm{NP}}(0)}{M_Z^2}$$

$$\alpha(M_Z^2) U^{\mathrm{NP}} = 4s_W^2 \left[\frac{\Pi_{WW}^{\mathrm{NP}}(M_W^2) - \Pi_{WW}^{\mathrm{NP}}(0)}{M_W^2} - c_W^2 \left(\frac{\Pi_{ZZ}^{\mathrm{NP}}(M_Z^2) - \Pi_{ZZ}^{\mathrm{NP}}(0)}{M_Z^2} \right) \right.$$

$$\left. -2s_W c_W \frac{\Pi_{\gamma Z}^{\mathrm{NP}}(M_Z^2)}{M_Z^2} - s_W^2 \frac{\Pi_{\gamma\gamma}^{\mathrm{NP}}(M_Z^2)}{M_Z^2} \right],$$

(2.4)

where $s_W^2 = \sin^2\theta_W = 1 - c_W^2 \equiv 1 - M_W^2/M_Z^2$, M_Z and M_W are, respectively, the Z boson and W boson masses. By comparing the measurable electroweak observables with the theory prediction one finds the fitted values [29]

$$\Delta S = S - S_{\rm SM} = 0.04 \pm 0.10$$
$$\Delta T = T - T_{\rm SM} = 0.05 \pm 0.11$$
$$\Delta U = U - U_{\rm SM} = 0.08 \pm 0.11 \tag{2.5}$$

for the reference Higgs and top masses $M_{H,\rm ref} = 120\,{\rm GeV}$ and $m_{t,\rm ref} = 173\,{\rm GeV}$, with the associated correlation matrix

$$V = \begin{pmatrix} 1 & +0.89 & -0.45 \\ +0.89 & 1 & -0.69 \\ -0.45 & -0.69 & 1 \end{pmatrix}. \tag{2.6}$$

We will include these constraints in our models by minimizing the χ^2 function defined as

$$\chi^2 = \sum_{i,j}(X_i^{\rm NP} - X_i)(\sigma^2)_{ij}^{-1}(X_j^{\rm NP} - X_j), \tag{2.7}$$

where $X_i = \Delta S, \Delta T, \Delta U$, are the fitted values of the oblique parameters with their corresponding uncertainties σ_i defined in eq. (2.5), $X_i^{\rm NP} = S^{\rm NP}, T^{\rm NP}, U^{\rm NP}$ are the contributions from the extra states that we will be introduced in each model investigated and $\sigma_{i,j}^2 \equiv \sigma_i V_{ij} \sigma_j$. We will allow the values of the parameters of our models to vary such that $\Delta\chi^2 = (3.53, 7.81, 11.3)$, which correspond to (68%, 95%, 99%) CL in a three-parameter fit. Since the difference between $M_{H,\rm ref}$ and the actual Higgs mass $M_H = 125\,{\rm GeV}$ is rather small and the uncertainties in the fitted parameters large, we will not correct for the exact result of the Higgs contribution to the oblique parameters.

Finally, since the new fermions couple to Z and γ they can be pair-produced at the LHC. We will examine, in each case, the production cross-section and comment on possible existing limits and perspectives. In order to calculate the production cross sections we have implemented our models in CalcHEP [30].

3   New fermion states

The existence of a chiral 4th generation that couples to the Higgs boson is excluded by data, since heavy quarks would contribute to the Higgs production cross section, increasing its rate by a factor ~ 9, and would exclude the Higgs up to $600\,{\rm GeV}$ [31]. In this work, we will deal with colorless vector-like fermions, so we do not have to worry about that. We will also assume that our fermions will have some new quantum number that forbids mixing with the usual SM fermions. In this case, we need to introduce at least two extra fermion fields in order to be able to build a renormalizable coupling term with the SM Higgs field and to have mixing. We will examine here the two smallest representations, see table 1. Let us stress that the triplet-doublet case with $y = 1/2$ corresponds to the supersymmetric Wino-Higgsino case.

Field	SU(2)$_L$ doublet-singlet	SU(2)$_L$ triplet-doublet	U(1)$_Y$
$\chi_{L,R}$	2	3	$\hat{y} = y - \frac{1}{2}$
$\psi_{L,R}$	1	2	y

Table 1. Representations of the new fermions and their corresponding hypercharges for the two cases we consider in this work.

3.1 Doublet-singlet model

The lagrangian describing the new fermion masses and couplings with the Higgs is

$$-\mathcal{L}_{\mathrm{H}}^{2+1} = c\,\overline{\psi_R}\,H\chi_L + c\,\tilde{H}\,\overline{\chi_R}P_L\psi_L + m_1\overline{\chi_R}P_L\chi_L + m_2\overline{\psi_R}P_L\psi_L + \text{h.c.}, \qquad (3.1)$$

where $\tilde{H} = i\tau_2 H^*$, c is the Yukawa coupling to the Higgs, $P_{L,R} = \frac{1}{2}(1 \pm \gamma_5)$, $m_{1,2}$ are the vector-like χ, ψ masses.

After electroweak symmetry breaking, the Higgs acquires a vacuum expectation value (vev) v endowing an extra mass contribution to the new fermions. The new fermions mass matrix takes the form

$$M_{2+1} = (\bar{\psi}_R \ \bar{\chi}_R^u \ \bar{\chi}_R^d) \begin{pmatrix} m_2 & cv & 0 \\ cv & m_1 & 0 \\ 0 & 0 & m_1 \end{pmatrix} \begin{pmatrix} \psi_L \\ \chi_L^u \\ \chi_L^d \end{pmatrix}, \qquad (3.2)$$

where we explicitly write the vector doublet as

$$\chi = \begin{pmatrix} \chi^u \\ \chi^d \end{pmatrix} \qquad (3.3)$$

To diagonalize M_{2+1} we introduce the following transformations

$$\omega_{L,R} \equiv \begin{pmatrix} \omega_{L,R}^1 \\ \omega_{L,R}^2 \end{pmatrix} = U_{L,R}^\dagger \begin{pmatrix} \psi_{L,R} \\ \chi_{L,R}^u \end{pmatrix} \qquad (3.4)$$

where $U_{L,R}$ are unitary matrices, so defining the three mass eigenstates: ω^1, ω^2 and χ^d with masses

$$M_{\omega_1,\omega_2} = \frac{1}{2}\left[(m_1 + m_2) \mp \sqrt{(m_2 - m_1)^2 + 4c^2v^2}\right] \quad \text{and} \quad M_\chi = m_1, \qquad (3.5)$$

$M_{\omega_1} < M_\chi < M_{\omega_2}$, in most of the parameter space.

The gauge interactions with the SM fields are described by the usual coupling with the SM fields are introduced via covariant derivatives

$$\mathcal{L}_{\mathrm{I}}^{2+1} = i\overline{\psi}\gamma^\mu\left(\partial_\mu - ig'y\,B_\mu\right)\psi + i\bar{\chi}\gamma^\mu\left(\partial_\mu - ig\,W_\mu^a T^a - ig'\hat{y}\,B_\mu\right)\chi, \qquad (3.6)$$

where $g' = e/c_W$, $g = e/s_W$ are the SM couplings. One can show that the neutral current lagrangian will be

$$\mathcal{L}_{\mathrm{NC}}^{2+1} = e \left(\hat{y} - \frac{1}{2} \right) \bar{\chi}^d \gamma_\mu \chi^d A^\mu + \left(-\hat{y}g' s_W - \frac{1}{2} g c_W \right) \bar{\chi}^d \gamma_\mu \chi^d Z^\mu$$

$$+ \bar{\omega} \left[U_L^\dagger \begin{pmatrix} -(\hat{y} + \frac{1}{2})g' s_W & 0 \\ 0 & \frac{g}{2}c_W - \hat{y}g' s_W \end{pmatrix} U_L P_L + (L \to R) \right] \gamma_\mu \omega Z^\mu$$

$$+ e \left(\hat{y} + \frac{1}{2} \right) \bar{\omega} \gamma_\mu \omega A^\mu, \tag{3.7}$$

and the charged current one

$$\mathcal{L}_{\mathrm{CC}}^{2+1} = \frac{g}{\sqrt{2}} \bar{\omega} \gamma^\mu \left[U_L^\dagger P_L + U_R^\dagger P_R \right] \widetilde{W}_\mu^{+T} \chi^d + \mathrm{h.c.}, \tag{3.8}$$

where we define $\widetilde{W}_\mu^+ \equiv (0 \quad W_\mu^+)$.

3.2 Triplet-doublet model

We will consider the following mass lagrangian for the new states

$$-\mathcal{L}_{\mathrm{mass}}^{3+2} = c \left(\overline{\psi_R} \chi_L H + \overline{\psi_L} \chi_R H \right) + m_1 \overline{\chi}_L \chi_R + m_2 \overline{\psi}_L \psi_R + \mathrm{h.c.}, \tag{3.9}$$

where c is their coupling to the SM Higgs field and m_1 and m_2 their vector-like masses. This gives rise, after electroweak symmetry breaking, to the following mass matrix

$$M_{3+2} = (\bar{\psi}_R^u \; \bar{\chi}_R^a \; \bar{\psi}_R^d \; \bar{\chi}_R^b \; \bar{\chi}_R^c) \begin{pmatrix} m_2 & cv & 0 & 0 & 0 \\ cv & m_1 & 0 & 0 & 0 \\ 0 & 0 & m_2 & -c\frac{v}{\sqrt{2}} & 0 \\ 0 & 0 & -c\frac{v}{\sqrt{2}} & m_1 & 0 \\ 0 & 0 & 0 & 0 & m_1 \end{pmatrix} \begin{pmatrix} \psi_L^u \\ \chi_L^a \\ \psi_L^d \\ \chi_L^b \\ \chi_L^c \end{pmatrix}, \tag{3.10}$$

where the doublet and triplet read

$$\psi = \begin{pmatrix} \psi^u \\ \psi^d \end{pmatrix}, \qquad \chi = \begin{pmatrix} \frac{\chi^b}{\sqrt{2}} & \chi^a \\ \chi^c & \frac{\chi^b}{\sqrt{2}} \end{pmatrix}. \tag{3.11}$$

To diagonalize M_{3+2} we introduce the following transformations

$$\omega_{L,R} \equiv \begin{pmatrix} \omega_{L,R}^1 \\ \omega_{L,R}^2 \end{pmatrix} = U_{L,R}^\dagger \begin{pmatrix} \psi_{L,R}^u \\ \chi_{L,R}^a \end{pmatrix} \qquad \xi_{L,R} \equiv \begin{pmatrix} \xi_{L,R}^1 \\ \xi_{L,R}^2 \end{pmatrix} = V_{L,R}^\dagger \begin{pmatrix} \psi_{L,R}^d \\ \chi_{L,R}^b \end{pmatrix} \tag{3.12}$$

where $U_{L,R}, V_{L,R}$ are unitary matrices, so defining the five mass eigenstates: ω^1, ω^2, ξ^1, ξ^2 and $\chi = \chi^c$ with masses

$$M_{\omega_1, \omega_2} = \frac{1}{2} \left[(m_1 + m_2) \mp \sqrt{(m_2 - m_1)^2 + 4c^2 v^2} \right]$$

$$M_{\xi_1, \xi_2} = \frac{1}{2} \left[(m_1 + m_2) \mp \sqrt{(m_2 - m_1)^2 + 2c^2 v^2} \right]$$

$$M_\chi = m_1 \tag{3.13}$$

$M_{\omega_1} < M_{\xi_1} < M_\chi < M_{\omega_2} < M_{\xi_2}$, in most of the parameter space.

The gauge interactions with the SM fields are described again in the usual way by

$$\mathcal{L}_\mathrm{I}^{3+2} = i\overline{\psi}\gamma^\mu \left(\partial_\mu - ig\, W_\mu^a T^a - ig'y\, B_\mu\right)\psi + i\bar{\chi}\gamma^\mu\left(\partial_\mu - igW_\mu^a T^a - ig'\hat{y}\, B_\mu\right)\chi, \quad (3.14)$$

giving rise to the neutral current lagrangian

$$\begin{aligned}
\mathcal{L}_\mathrm{NC}^{3+2} =\;& e(\hat{y}-1)\,\bar{\chi}\gamma_\mu\chi\, A^\mu + \left(-g'\,\hat{y}\,s_W - g\,c_W\right)\bar{\chi}\gamma_\mu\chi\, Z^\mu \\
&+\bar\omega\left[U_L^\dagger\begin{pmatrix} \tfrac{g}{2}\,c_W - yg'\,s_W & 0 \\ 0 & g\,c_W - \hat{y}g'\,s_W \end{pmatrix}U_L P_L + (L\to R)\right]\gamma_\mu\omega\, Z^\mu \\
&+(\hat{y}+1)\,e\,\bar\omega\gamma_\mu\,\omega A^\mu \\
&+\bar\xi\left[V_L^\dagger\begin{pmatrix} -\tfrac{g}{2}\,c_W - yg'\,s_W & 0 \\ 0 & -\hat{y}\,g'\,s_W \end{pmatrix}V_L P_L + (L\to R)\right]\gamma_\mu\xi\, Z^\mu \\
&+\hat{y}\,e\,\bar\xi\gamma_\mu\xi\, A^\mu,
\end{aligned} \qquad (3.15)$$

and to the charged current lagrangian

$$\mathcal{L}_\mathrm{CC}^{3+2} = g\left(\bar\omega\ \bar\xi\ \bar\chi\right)\gamma^\mu\left[\begin{pmatrix} 0_{2\times2} & W_\mu^+ U_L^\dagger V_L' & 0_{2\times1} \\ W_\mu^- V_L'^\dagger U_L & 0_{2\times2} & V_L^\dagger \widetilde{W}_\mu^{+T} \\ 0_{1\times2} & \widetilde{W}_\mu^- V_L & 0 \end{pmatrix}P_L + (L\to R)\right]\begin{pmatrix}\omega \\ \xi \\ \chi\end{pmatrix}, \quad (3.16)$$

where $0_{n\times m}$ is a $n\times m$ zero matrix, $\widetilde{W}_\mu^- \equiv (0\ \ W_\mu^-)$, $\widetilde{W}_\mu^+ \equiv (0\ \ W_\mu^+)$ and

$$V_L' = \frac{1}{\sqrt{2}}\begin{pmatrix} V_{11L} & V_{12L} \\ \sqrt{2}\,V_{21L} & \sqrt{2}\,V_{22L} \end{pmatrix}. \qquad (3.17)$$

4 $H \to \gamma\gamma$ width

We have studied the Higgs to diphoton width in the doublet-singlet model and in the triplet-doublet model. In both models the ratio

$$R_{\gamma\gamma} = \frac{\Gamma(H\to\gamma\gamma)}{\Gamma^\mathrm{SM}(H\to\gamma\gamma)}, \qquad (4.1)$$

between the width of $H \to \gamma\gamma$ with extra states and the width of $H \to \gamma\gamma$ in the SM have the feature that fixing the lightest new fermion mass the largest enhancement[1] will be achieved for $m_1 = m_2$. This is illustrated in figure 1. These plots also show the symmetry between m_1 and m_2 that can be also seen from eqs. (3.5) and (3.13).

In figure 2 we show the allowed regions at 68%, 95% and 99% CL, according to ref. [3], for the ratio $R_{\gamma\gamma}$ in the plane $(m_1 = m_2)\times c$ for the doublet-singlet model and for several ω charges. We also show some iso-lines corresponding to the mass of the lightest new particle, either ω_1 or ω_2, depending on the parameter values. We will simply call this lightest mass

---

[1]One may wonder that a large enhancement in $H \to \gamma\gamma$ may induce a deviation of some production cross sections, specially vector boson fusion (VBF). Nevertheless, the top loop corrections to VBF is $\mathcal{O}(\text{few }\%)$, so we do not expect a large departure from the SM cross section.
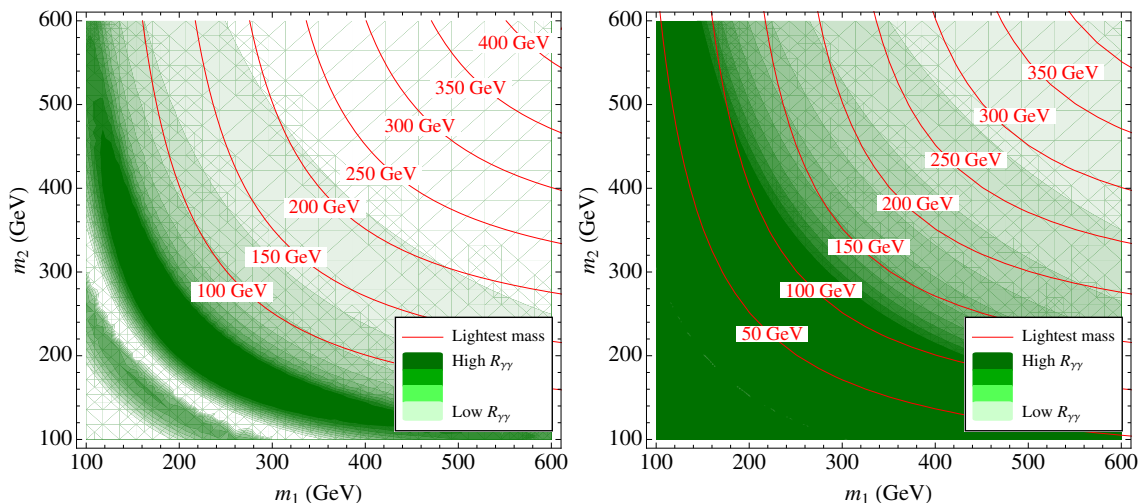
Figure 1. Iso-contours of the ratio $R_{\gamma\gamma}$ in the plane m_1 versus m_2 for $c = 1$. We also show in the same plot the iso-lines that correspond to a fixed value of the lightest new charged fermion mass. The doublet-singlet model behavior with $y = 1$ is illustrated on the left and the triplet-doublet model with $y = -5/2$ on the right panel.

M_{light}. The region where $M_{\text{light}} \lesssim 100\,\text{GeV}$ is already excluded by LEP data [32]. As a reference we also display some iso-lines for fixed values of $R_{\gamma\gamma}$.
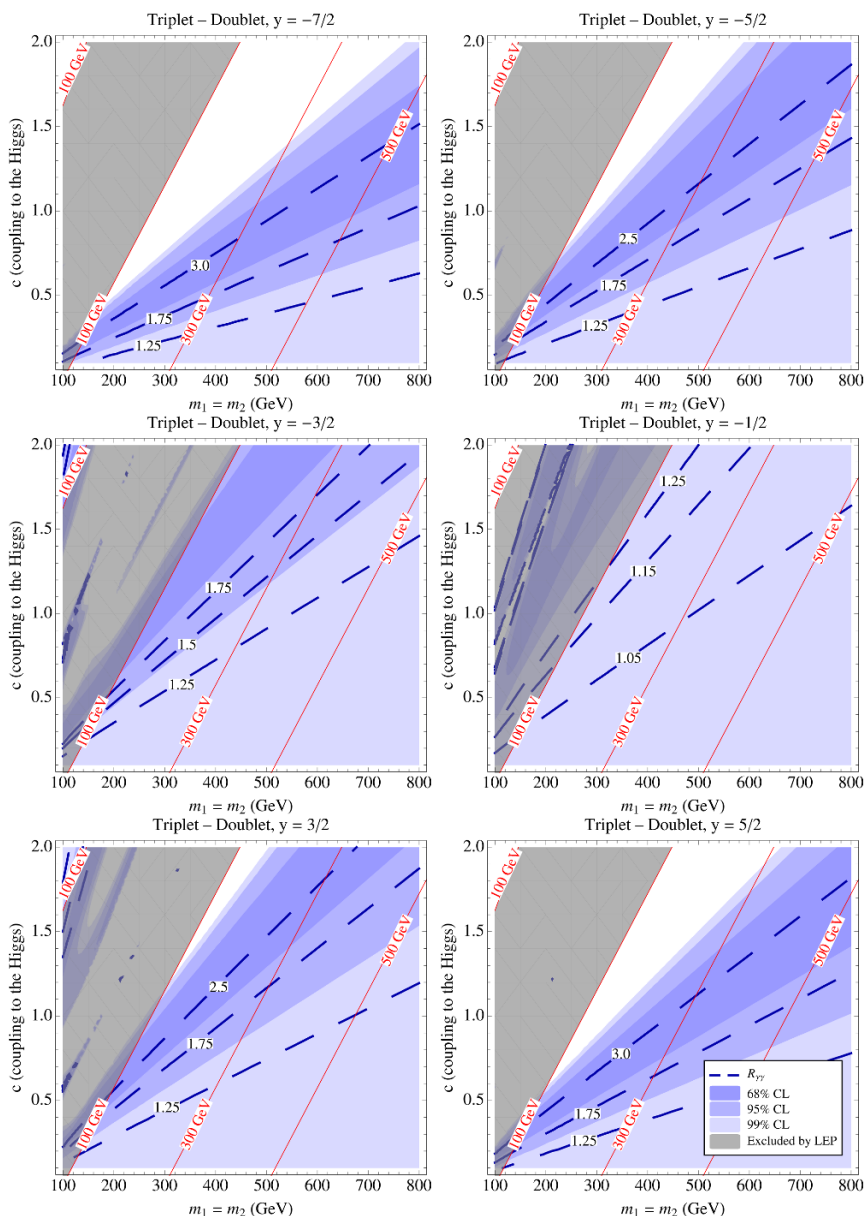
In the doublet-singlet model there is only one electric charge at play in the extra states contribution, so there is no sensitivity to the sign of the charge. However, as m_1, m_2 and c vary one can have a complete cancellation of their contribution to $H \to \gamma\gamma$, and for a small parameter region, even have a smaller $\Gamma(H \to \gamma\gamma)$ that the SM one. For this reason, we have two disconnected regions that are consistent with the allowed range of $R_{\gamma\gamma}$. On the top panel of figure 2 those two regions are very close together and for the most part concentrated at $M_{\text{light}} \lesssim 100\,\text{GeV}$. As we increase the absolute charge of ω we start to see these regions being pulled apart and away from $M_{\text{light}} \lesssim 100\,\text{GeV}$ (see middle panel of figure 2) until one of the regions disappear from the plot.

For a coupling to the Higgs of $\mathcal{O}(1)$, hypercharge $y = 1$ and $M_{\text{light}} > 100\,\text{GeV}$ there is compatibility only if the future LHC data show a decrease of $\Gamma(H \to \gamma\gamma)$ to a value at most 25% higher than the SM one, i.e., in the 99% CL allowed region by the current LHC data. For $y > 1$ there are solutions even inside the 68% CL, for M_{light} that can be as high as a few hundred of GeV, well inside the LHC discovery reach.

In figure 3 we show the allowed regions at 68%, 95% and 99% CL, according to ref. [3], for the ratio $R_{\gamma\gamma}$ in the plane $(m_1 = m_2) \times c$ for the triplet-doublet model and for several ω charges. We also show some iso-lines corresponding to the mass for the lightest new particle, eitheir ω_1 or ξ_1, depending on the parameter values. Again we will call this lightest mass M_{light}. The region where $M_{\text{light}} \lesssim 100\,\text{GeV}$ is already excluded by LEP data [32]. As a reference we also display some iso-lines for fixed $R_{\gamma\gamma}$.

In the triplet-doublet model there are four states and two different electric charges at play, so different charge combinations will give rise to a more interesting behavior. As

Figure 2. Regions in the plane $(m_1 = m_2) \times c$ allowed by the fit to the combined Higgs data for $R_{\gamma\gamma}$, according to ref. [3] at 68% (darker blue), 95% (intermediate blue) and 99% (lighter blue) CL, for the doublet-singlet model. We also show some iso-lines of constant mass for the lightest new particle, M_{light}, depending on the parameter values. The region excluded by LEP, for $M_{\text{light}} \lesssim 100\,\text{GeV}$, is shown in grey. As a reference we also show some isolines that correspond to $R_{\gamma\gamma} = 1.25, 1.5, 1.75, 2.0$ and 3.0. On the top, middle and lower panels we show the cases $y = 1, 2$ and 3, which corresponds to ω with charge ± 1, ± 2 and ± 3, respectively.

Figure 3. Regions in the plane $(m_1 = m_2) \times c$ allowed by the fit to the combined Higgs data for $R_{\gamma\gamma}$, according to ref. [3] at 68% (darker blue), 95% (intermediate blue) and 99% (lighter blue) CL, for the triplet-doublet model. We also show some iso-lines of constant mass for the lightest new particle, M_{light}, depending on the parameter values. The region excluded by LEP, for $M_{\text{light}} \lesssim 100 \, \text{GeV}$, is shown in grey. As a reference we also show some isolines that correspond to $R_{\gamma\gamma} = 1.05, 1.15, 1.25, 1.5, 1.75$ and 2.5. On the top panel we show on the left (right) the case $y = -7/2$ ($y = -5/2$) that correspond to ω and ξ with charges -3 and -4 (-2 and -3), respectively. On the middle panel we show on the left (right) the case $y = -3/2$ ($y = -1/2$) that correspond to ω and ξ with charges -1 and -2 (0 and -1), respectively. On the lower panel we show on the left (right) the case $y = 3/2$ ($y = 5/2$) that correspond to ω and ξ with charges 2 and 1 (3 and 2), respectively.
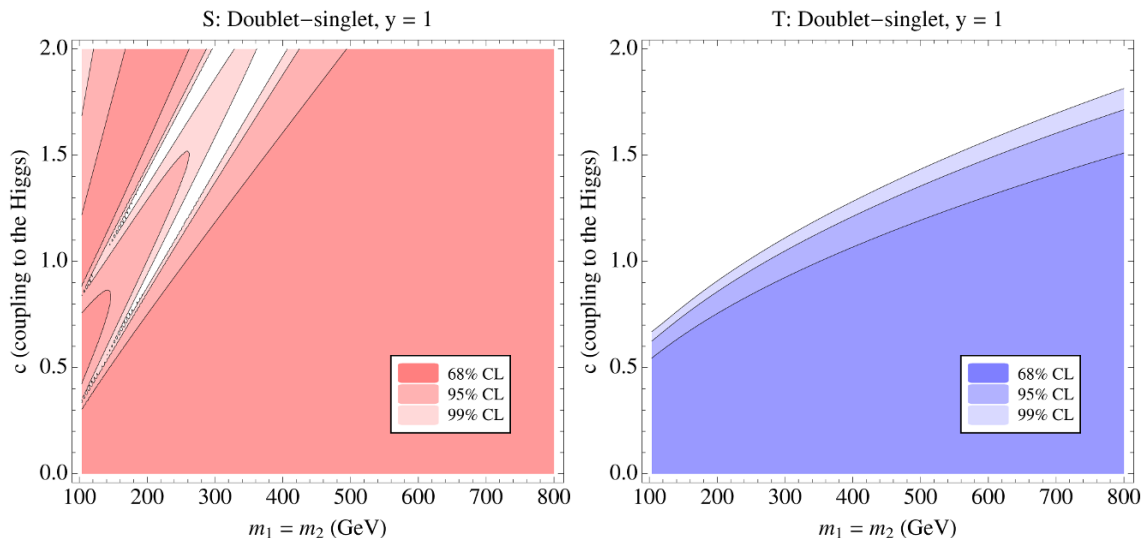
Figure 4. Allowed regions for S (left panel) and T (right panel) in the plane $m_1 = m_2$ versus c, the coupling to the Higgs for the doublet-singlet model with $y = 1$.

before, and for the same reasons explained above, we have two disconnected regions that are consistent with the allowed $R_{\gamma\gamma}$. However, as we increase the charges these regions swap places.

In figure 3, the charges of (ω, ξ) are, respectively, from left to right and top to bottom, $(-3, -4), (-2, -3), (-1, -2), (0, -1), (2, 1)$ and $(3, 2)$. For large negative charges we can see only one of those regions (top panels). As we increase the charges, we start to see both regions, although most of the second allowed region is forbidden by the LEP limit (middle panels). Finally the two regions crossover and swap places (bottom panels). We do not show here the case $y = 1/2$ because it is almost exactly the same as the top panel of figure 2, since ω have charge 1 and ξ charge 0 in this case.

For a coupling to the Higgs of $\mathcal{O}(1)$, the compatibility region where there is a solution for $R_{\gamma\gamma}$ at 68% and 95% CL strongly depends on the y value. Again the lightest particle can be within the LHC discovery range.

5 Oblique parameters S and T

We now examine the contributions of these new states to the oblique parameters. In figure 4 we show the allowed regions at 68%, 95% and 99% CL for S (left panel) and T (right panel) for the doublet-singlet model with $y = 1$ to illustrate the S and T separate behavior. We do not show a plot for U, since it poses practically no additional bound on the parameter space. S has two preferred regions, reflecting the same degeneracy we have seen before for $R_{\gamma\gamma}$. T, for $c \lesssim 0.5$ allows for any values of $m_1 = m_2$, but as c increases lower values of $m_1 = m_2$ become forbidden. This is because T is sensitive to the mass splitting of the doublet and prefers thus smaller mixing.

In figure 5 we show the the allowed regions at 68%, 95% and 99% CL for S (left panel) and T (right panel) for the triplet-doublet model for $y = -5/2$ to illustrate the S and T
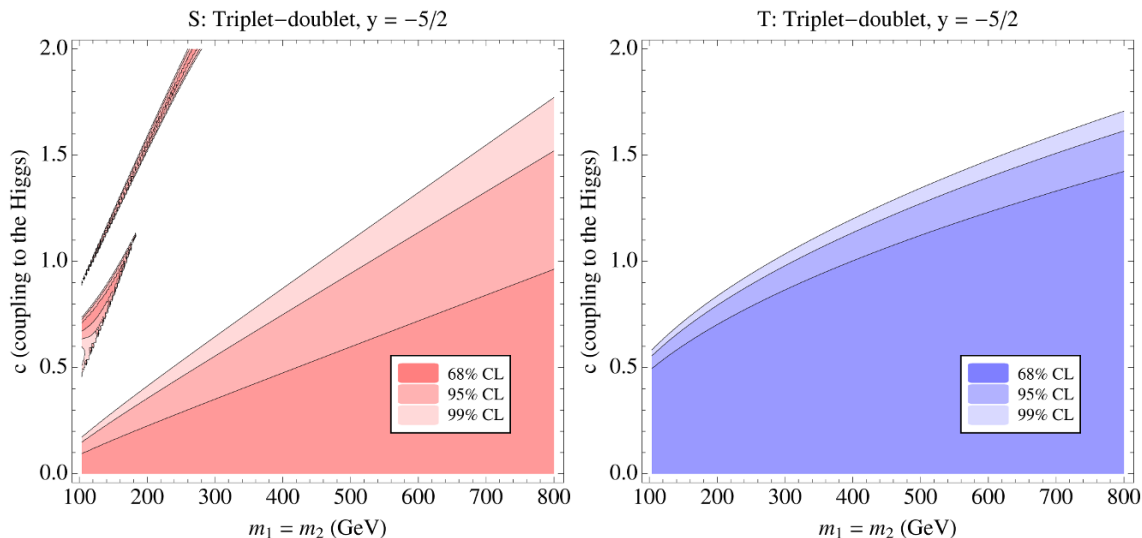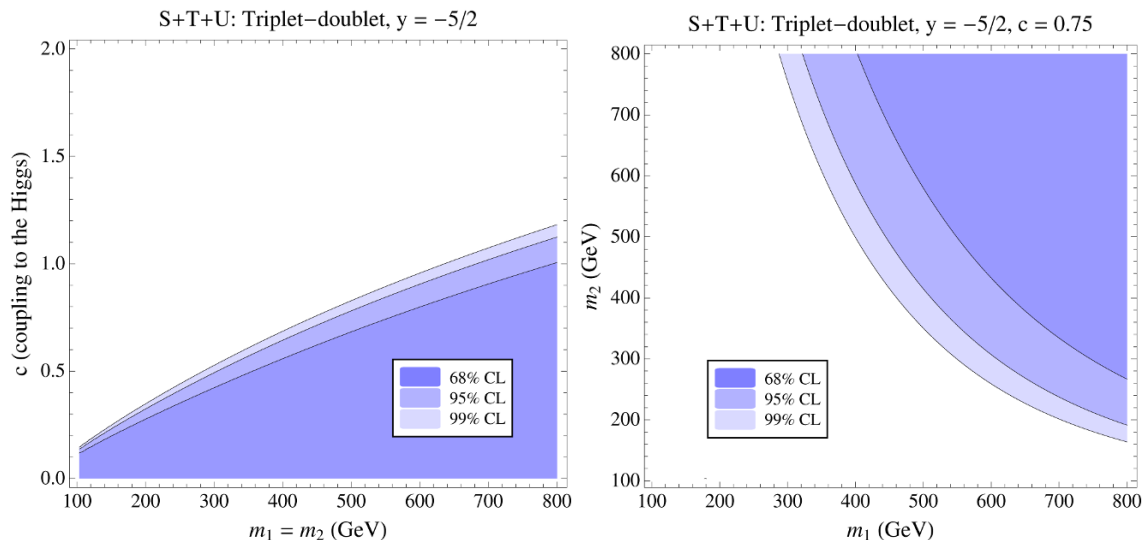
Figure 5. Allowed regions for S (left panel) and T (right panel) in the plane $m_1 = m_2$ versus c, the coupling to the Higgs for the triplet-doublet model with $y = -5/2$.
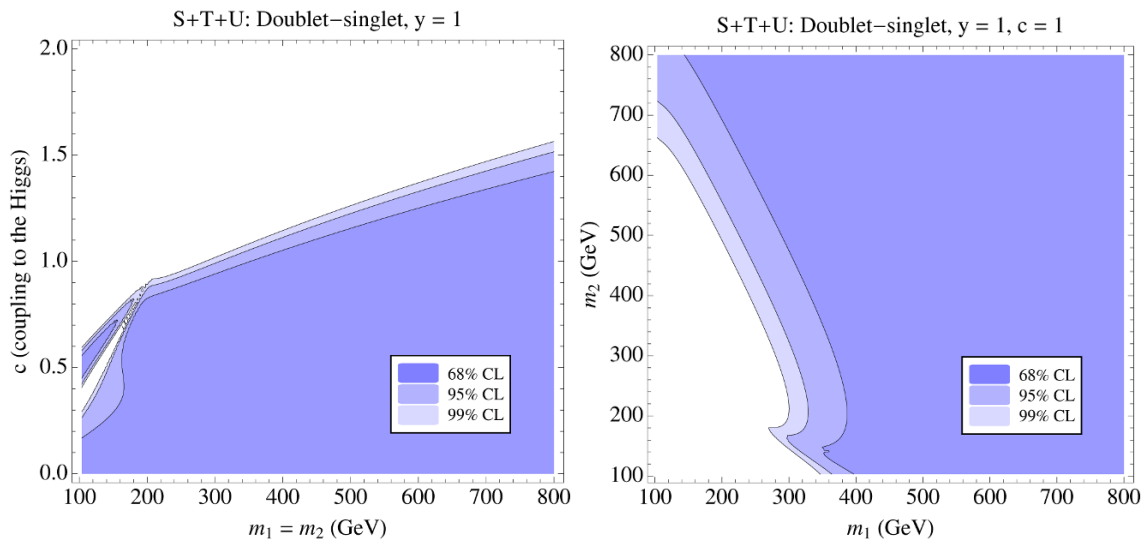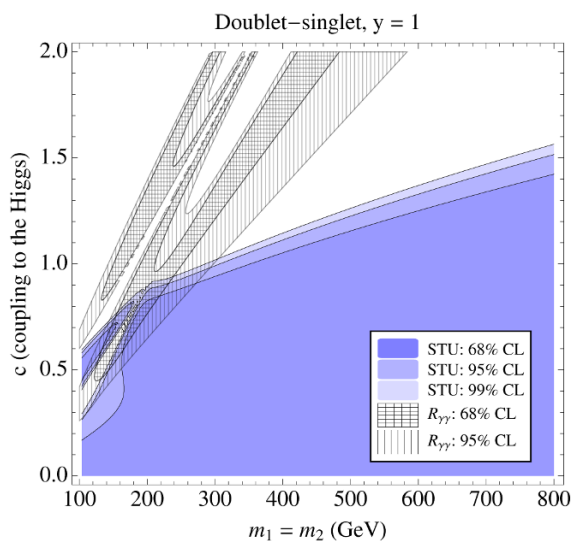

Figure 6. Allowed region for the combined fit of S, T and U for $y = 1$ and $m_1 = m_2$ (left panel) and for $y = 1$ and $c = 1$ (right panel) in the doublet-singlet model.

separate behavior. Again, we do not show a separate plot for U. Here the second S region becomes a thin strip, while for T the behavior is very similar to the doublet-singlet case.

Now we will combine S and T using the χ^2 function described in eq. (2.7) of section 2 allowing for correlations. In figure 6 we show the combined region allowed for the fit of S and T for $y = 1$ and $m_1 = m_2$ (left panel) and for $c = y = 1$ (right panel) for the doublet-singlet case. When we compare this with with figure 4 we see that the T parameter pulls the combined allowed region down. The plot on the right also shows the correlation between m_1 and m_2 allowed by T. In figure 7 we show the combined region allowed for the fit of S and T for $y = -5/2$ and $m_1 = m_2$ (left panel) and for $c = 1$ and $y = -5/2$ (right panel) for the triplet-doublet case.
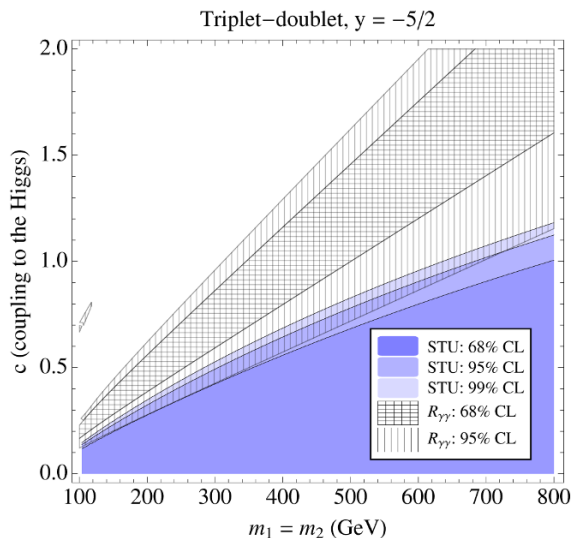
Figure 7. Allowed region for the combined fit of S, T and U for $y = -5/2$ and $m_1 = m_2$ (left panel) and for $y = -5/2$ and $c = 0.75$ (right panel) in the triplet-doublet model.

Figure 8. Allowed region for the combined fit of S and T for $y = 1$ in the doublet-singlet model and its compatibility to $R_{\gamma\gamma}$. We show the $R_{\gamma\gamma}$ allowed regions at 68% and 95% CL.

In figure 8 we see that for the case where $y = 1$ there is great tension between the region that is preferred by $R_{\gamma\gamma}$ and the region allowed by S and T parameters. This is expected because T prefers a region where there is a small breaking of $\mathrm{SU}(2)_L$ while $R_{\gamma\gamma}$ is mostly enhanced for large mixing. The same general behavior can be observed in figure 9 for $y = -5/2$ in the triplet-doublet model, although in this case, the tension is alleviated.

Figure 9. Allowed region for the combined fit of S and T for $y = -5/2$ in the triplet-doublet model and its compatibility to $R_{\gamma\gamma}$. We show the $R_{\gamma\gamma}$ allowed regions at 68% and 95% CL.

6 Production at the LHC

These new charged states could be produced at the LHC and we have calculated the cross section for pair production of the lightest fermion in the doublet-singlet model, and correspondingly in the triplet-doublet model.

This was done for p-p collisions at the LHC running at a center of mass energy of 8 TeV, using CalcHEP [30] with CTEQ6L [34] parton distribution functions for the proton and imposing the following loose cuts: $-2.1 < \eta < 2.1$ and $p_T > 40$ GeV for each fermion.

For both models, the main contributions to pair production of the lightest particle come from neutral currents Z and γ exchange in the s channel.

In figure 10 the results of our calculations for the production cross section as a function of the mass of the lightest particle, for $y = 1$ for the doublet-singlet model and $y = -3/2$ for the doublet-triplet model. We also include in figure 10, the current bounds on the cross-section on stau from CMS [33].

These stringent bounds in the lower mass region could lead to some indication of the possible charges of these new fermions. For example, for masses > 300 GeV, together with the electroweak precision tests, figures 2 and 3 point to specific charges that are preferred for the current allowed regions of $R_{\gamma\gamma}$. Additional structure to this sector, on the other hand, could permit one to evade them.

7 Conclusions

We have investigated how the addition of extra uncolored fermion states which do not mix to the Standard Model fermions, but do couple to the Higgs, and therefore affects the $H \to \gamma\gamma$ rate. We focus on the two smallest possibilities for the $SU(2)_L$ representation of the fermion fields that can give rise to a renormalizable lagrangian, coupling it to the
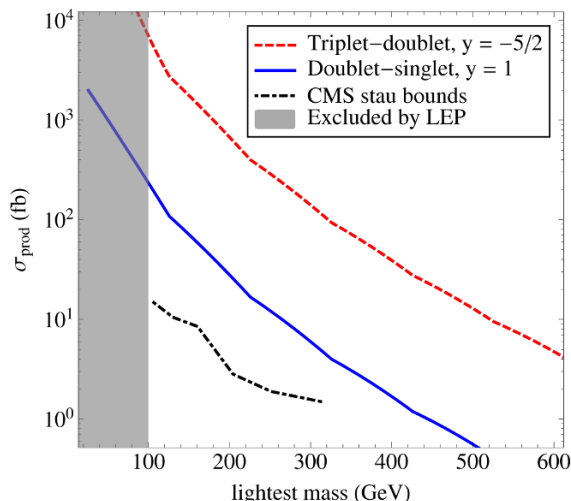
Figure 10. Pair production cross section for the lightest new state in the doublet-singlet model with $y = 1$ and in the triplet-doublet model with $y = -5/2$. We also show the CMS limit for long lived staus pair production [33] at 7 TeV.

Higgs, and contributing to the Higgs diphoton width: the doublet-singlet model and the triplet-double model.

We map the masses, charges and couplings that these possible states must have in order to satisfy the current limits on $\Gamma(H \to \gamma\gamma)$ from the LHC and the Tevatron Higgs combined data [3] and confront them with the allowed ones from electroweak precision measurements.

We computed the pair production cross-section for the lightest states and compared it to the current bounds from long-lived charged particles.

Acknowledgments

Note added. During the finalization of this paper ref. [35, 36] appeared.

A   Definitions of some functions used in this work

Here we for completeness we define the loop functions used to compute $\Gamma(H \to \gamma\gamma)$.

$$A_1(\tau) = -[2\tau^2 + 3\tau + 3(2\tau - 1)g(\tau)]/\tau^2 \tag{A.1}$$

$$A_{1/2}(\tau) = 2[\tau + (\tau - 1)g(\tau)]/\tau^2 \tag{A.2}$$

$$A_0(\tau) = -[\tau - g(\tau)]/\tau^2 \tag{A.3}$$

where $g(\tau) = \arcsin^2 \sqrt{\tau}$, for $\tau \leq 1$.

For the fermion gauge boson interaction lagrangian that can be generically written as

$$\mathcal{L}_{V f_i f_j} = \bar{f}_i (g_{LV}^{ij} P_L + g_{RV}^{ij} P_R) \gamma_\mu f_j V^\mu$$

we define the two point functions that enter in the oblique parameters calculation in terms of the generic couplings and of the universal functions $\Pi_{V \pm A}$ as [19, 37]

$$\Pi_{V_1 V_2}(s) = (g_{LV_1}^{ij} g_{LV_2}^{ij} + g_{RV_1}^{ij} g_{RV_2}^{ij}) \Pi_{V+A}(s, m_i, m_j) + (g_{LV_1}^{ij} g_{RV_2}^{ij} + g_{LV_2}^{ij} g_{RV_1}^{ij}) \Pi_{V-A}(s, m_i, m_j), \tag{A.4}$$

where a sum is implicit over all fermions involved, $V_1, V_2 = W, Z, \gamma$, m_i and m_j are the masses of the fermions f_i and f_j in the loop and

$$\begin{aligned}
\Pi_{V+A}(s, m_i, m_j) = \frac{N_c}{24\pi^2} &\left[m_i^2 \ln m_i^2 \left(1 - \frac{(m_i^2 - m_j^2)}{2s} \right) + m_j^2 \ln m_j^2 \left(1 - \frac{(m_j^2 - m_i^2)}{2s} \right) \right. \\
&+ \left(s - \frac{(m_i^2 + m_j^2)}{2} - \frac{(m_i^2 - m_j^2)^2}{2s} \right) \left(\bar{B}_0(s, m_i, m_j) - \ln(m_i m_j) \right) \\
&\left. - \frac{s}{3} + \frac{(m_i^2 - m_j^2)^2}{2s} + \Delta_{\text{div}} \right],
\end{aligned} \tag{A.5}$$

and

$$\Pi_{V-A}(s, m_i, m_j) = \frac{N_c}{8\pi^2} m_i m_j \left(\bar{B}_0(s, m_i, m_j) - \ln(m_i m_j) + \Delta_\epsilon \right), \tag{A.6}$$

here N_c are the number of colors, the divergent part $\Delta_{\text{div}} \equiv \Delta_\epsilon (s - \frac{3}{2}(m_i^2 + m_j^2))$ with $\Delta_\epsilon = \frac{2}{\epsilon} - \gamma + \ln 4\pi + \ln \mu^2$.

We have used the finite part of the B_0 function

$$\bar{B}_0(s, m_i, m_j) = 1 - \frac{m_i^2 + m_j^2}{m_i^2 - m_j^2} \ln \left(\frac{m_i}{m_j} \right) + F(s, m_i, m_j), \tag{A.7}$$

with

$$F(s, m_i, m_j) = -1 + \frac{m_i^2 + m_j^2}{m_i^2 - m_j^2} \ln \left(\frac{m_i}{m_j} \right) - \int_0^1 dx \ln \left(\frac{x^2 - x(s + m_i^2 - m_j^2) + m_i^2 - i\epsilon}{m_i m_j} \right). \tag{A.8}$$

as defined in ref. [37]. Note that $F(0, m_i, m_j) = 0$ so that $\bar{B}_0(0, m, m) = 0$.

For $s = 0$, the finite part of the previous expressions reads

$$\Pi_{V+A}(0, m_i, m_j) = \frac{N_c}{24\pi^2} \frac{2m_i^4 (1 - 4 \ln m_i) - 2m_j^4 (1 - 4 \ln m_j)}{m_i^2 - m_j^2}, \tag{A.9}$$

$$\Pi_{V-A}(0, m_i, m_j) = \frac{N_c}{24\pi^2} \frac{8 m_i m_j \left(m_i^2 (2 \ln m_i - 1) - m_j^2 (2 \ln m_j - 1) \right)}{m_i^2 - m_j^2}. \tag{A.10}$$

References

[1] ATLAS collaboration, F. Gianotti, *Latest update in the search for the Higgs boson.* http://indico.cern.ch/conferenceDisplay.py?confId=197461 (2012).

[2] CMS collaboration, J. Incandela, *Latest update in the search for the Higgs boson,* http://indico.cern.ch/conferenceDisplay.py?confId=197461.

[3] T. Corbett, O. Eboli, J. Gonzalez-Fraile and M. Gonzalez-Garcia, *Constraining anomalous Higgs interactions, Phys. Rev.* **D 86** (2012) 075013 [arXiv:1207.1344] [INSPIRE].

[4] P.P. Giardino, K. Kannike, M. Raidal and A. Strumia, *Is the resonance at 125 GeV the Higgs boson?,* arXiv:1207.1347 [INSPIRE].

[5] J. Espinosa, C. Grojean, M. Muhlleitner and M. Trott, *First glimpses at Higgs' face,* arXiv:1207.1717 [INSPIRE].

[6] ATLAS collaboration, G. Aad et al., *Combined search for the standard model Higgs boson in pp collisions at $\sqrt{s} = 7$ TeV with the ATLAS detector, Phys. Rev.* **D 86** (2012) 032003 [arXiv:1207.0319] [INSPIRE].

[7] CMS collaboration, S. Chatrchyan et al., *Combined results of searches for the standard model Higgs boson in pp collisions at $\sqrt{s} = 7$ TeV, Phys. Lett.* **B 710** (2012) 26 [arXiv:1202.1488] [INSPIRE].

[8] CMS collaboration, *Evidence for a new state decaying into two photons in the search for the standard model Higgs boson in pp collisions,* PAS-HIG-12-015 (2012).

[9] CMS collaboration, *Observation of a new boson with a mass near 125 GeV,* PAS-HIG-12-020 (2012).

[10] ATLAS collaboration, *Observation of an excess of events in the search for the standard model Higgs boson in the γ-γ channel with the ATLAS detector,* ATLAS-CONF-2012-091 (2012).

[11] TEVATRON NEW PHYSICS HIGGS WORKING GROUP, CDF COLLABORATION, D0 collaboration, C. Group, D. Collaborations, the Tevatron New Physics and H. Working, *Updated combination of CDF and D0 searches for standard model Higgs boson production with up to $10.0\,fb^{-1}$ of data,* arXiv:1207.0449 [INSPIRE].

[12] CMS collaboration, S. Chatrchyan et al., *Search for the standard model Higgs boson decaying into two photons in pp collisions at $\sqrt{s}=7$ TeV, Phys. Lett.* **B 710** (2012) 403 [arXiv:1202.1487] [INSPIRE].

[13] ATLAS collaboration, G. Aad et al., *Search for the standard model Higgs boson in the diphoton decay channel with $4.9\,fb^{-1}$ of pp collisions at $\sqrt{s} = 7$ TeV with ATLAS, Phys. Rev. Lett.* **108** (2012) 111803 [arXiv:1202.1414] [INSPIRE].

[14] J. Cao, Z. Heng, T. Liu and J.M. Yang, *Di-photon Higgs signal at the LHC: a comparative study for different supersymmetric models, Phys. Lett.* **B 703** (2011) 462 [arXiv:1103.0631] [INSPIRE].

[15] A. Alves, E. Ramirez Barreto, A. Dias, C. de S. Pires, F. Queiroz, et al., *Probing 3-3-1 models in diphoton Higgs boson decay*, *Phys. Rev.* **D 84** (2011) 115004 [arXiv:1109.0238] [INSPIRE].

[16] M. Carena, S. Gori, N.R. Shah and C.E. Wagner, *A 125 GeV SM-like Higgs in the MSSM and the γγ rate*, *JHEP* **03** (2012) 014 [arXiv:1112.3336] [INSPIRE].

[17] P. Draper and D. McKeen, *Diphotons from tetraphotons in the decay of a 125 GeV Higgs at the LHC*, *Phys. Rev.* **D 85** (2012) 115023 [arXiv:1204.1061] [INSPIRE].

[18] K. Kumar, R. Vega-Morales and F. Yu, *Effects from new colored states and the Higgs portal on gluon fusion and Higgs decays*, arXiv:1205.4244 [INSPIRE].

[19] S. Dawson and E. Furlan, *A Higgs conundrum with vector fermions*, *Phys. Rev.* **D 86** (2012) 015021 [arXiv:1205.4733] [INSPIRE].

[20] M. Carena, S. Gori, N.R. Shah, C.E. Wagner and L.-T. Wang, *Light Stau phenomenology and the Higgs γγ rate*, *JHEP* **07** (2012) 175 [arXiv:1205.5842] [INSPIRE].

[21] A. Akeroyd and S. Moretti, *Enhancement of H to γγ from doubly charged scalars in the Higgs triplet model*, *Phys. Rev.* **D 86** (2012) 035015 [arXiv:1206.0535] [INSPIRE].

[22] D. Carmi, A. Falkowski, E. Kuflik and T. Volansky, *Interpreting the Higgs*, arXiv:1206.4201 [INSPIRE].

[23] M. Carena, I. Low and C.E. Wagner, *Implications of a modified Higgs to diphoton decay width*, *JHEP* **08** (2012) 060 [arXiv:1206.1082] [INSPIRE].

[24] D. Carmi, A. Falkowski, E. Kuflik, T. Volansky and J. Zupan, *Higgs after the discovery: a status report*, *JHEP* **10** (2012) 196 [arXiv:1207.1718] [INSPIRE].

[25] W.-F. Chang, J.N. Ng and J.M. Wu, *Constraints on new scalars from the LHC 125 GeV Higgs signal*, *Phys. Rev.* **D 86** (2012) 033003 [arXiv:1206.5047] [INSPIRE].

[26] D. Bertolini and M. McCullough, *The social Higgs*, arXiv:1207.4209 [INSPIRE].

[27] G. Altarelli and R. Barbieri, *Vacuum polarization effects of new physics on electroweak processes*, *Phys. Lett.* **B 253** (1991) 161 [INSPIRE].

[28] M.E. Peskin and T. Takeuchi, *Estimation of oblique electroweak corrections*, *Phys. Rev.* **D 46** (1992) 381 [INSPIRE].

[29] M. Baak, M. Goebel, J. Haller, A. Hoecker, D. Ludwig, et al., *Updated status of the global electroweak fit and constraints on new physics*, *Eur. Phys. J.* **C 72** (2012) 2003 [arXiv:1107.0975] [INSPIRE].

[30] A. Pukhov, *CalcHEP 2.3: MSSM, structure functions, event generation, batchs and generation of matrix elements for other packages*, hep-ph/0412191 [INSPIRE].

[31] CMS collaboration, *Inclusive search for a sequential fourth generation of quarks*, PAS-EXO-11-098 (2011).

[32] L3 collaboration, P. Achard et al., *Search for heavy neutral and charged leptons in e^+e^- annihilation at LEP*, *Phys. Lett.* **B 517** (2001) 75 [hep-ex/0107015] [INSPIRE].

[33] CMS collaboration, S. Chatrchyan et al., *Search for heavy long-lived charged particles in pp collisions at $\sqrt{s}=7$ TeV*, *Phys. Lett.* **B 713** (2012) 408 [arXiv:1205.0272] [INSPIRE].

[34] J. Pumplin, D. Stump, J. Huston, H. Lai, P.M. Nadolsky, et al., *New generation of parton distributions with uncertainties from global QCD analysis*, *JHEP* **07** (2002) 012 [hep-ph/0201195] [INSPIRE].

[35] A. Joglekar, P. Schwaller and C.E. Wagner, *Dark matter and enhanced Higgs to di-photon rate from vector-like leptons*, arXiv:1207.4235 [INSPIRE].

[36] N. Arkani-Hamed, K. Blum, R.T. D'Agnolo and J. Fan, *2:1 for naturalness at the LHC?*, arXiv:1207.4482 [INSPIRE].

[37] W.F.L. Hollik, *Radiative corrections in the standard model and their role for precision tests of the electroweak theory*, DESY-88-188 (1988).